

Wave packet molecular dynamics simulations of warm dense hydrogen

This article has been downloaded from IOPscience. Please scroll down to see the full text article.

2003 J. Phys. A: Math. Gen. 36 6165

(<http://iopscience.iop.org/0305-4470/36/22/344>)

View [the table of contents for this issue](#), or go to the [journal homepage](#) for more

Download details:

IP Address: 171.66.16.103

The article was downloaded on 02/06/2010 at 15:36

Please note that [terms and conditions apply](#).

Wave packet molecular dynamics simulations of warm dense hydrogen

M Knaup, P-G Reinhard, C Toepffer and G Zwicknagel

Institut für Theoretische Physik, Universität Erlangen, Staudtstr. 7, D-91058 Erlangen, Germany

E-mail: zwicknagel@theorie2.physik.uni-erlangen.de

Received 24 October 2002

Published 22 May 2003

Online at stacks.iop.org/JPhysA/36/6165

Abstract

Recent shock-wave experiments with deuterium [1, 2] in a regime where a plasma phase-transition has been predicted [3] and their theoretical interpretation are the matter of a controversial discussion (see e.g. [4–8]). In this paper, we apply ‘wave packet molecular dynamics’ (WPMD) simulations to investigate warm dense hydrogen. The WPMD method was originally used by Heller for a description of the scattering of composite particles such as simple atoms and molecules [9]; later it was applied to Coulomb systems by Klakow *et al* [10, 11]. In the present version of our model the protons are treated as classical point-particles, whereas the electrons are represented by a completely anti-symmetrized Slater sum of periodic Gaussian wave packets. We present recent results for the equation of state of hydrogen at constant temperature $T = 300$ K and of deuterium at constant Hugoniot $E - E_0 + \frac{1}{2}(\frac{1}{n} - \frac{1}{n_0})(p + p_0) = 0$, and compare them with the experiments and several theoretical approaches.

PACS numbers: 03.67.Lx, 05.30.-d, 71.10.-w

1. Introduction

The behaviour of hydrogen at Mbar pressure remains controversial and poses a fundamental challenge to experiment and theory. On the theoretical side, various complementary methods, such as, e.g., density functionals or path-integral Monte Carlo, are used to investigate hydrogen under these extreme conditions of temperature and density where quantum effects such as the wave nature of the particles and their indistinguishability are important. In the wave packet molecular dynamics (WPMD) method, which is based on a time-dependent variational principle, these quantum effects are approximately taken into account by representing the electrons by anti-symmetrized localized wave packets with a simple analytical form. The wave packet approach reproduces fairly well many dynamic properties of quantum many-body systems as has been shown by Heller for the scattering of composite particles such as

atoms and molecules [9], by Feldmeier for heavy ion scattering [12] and by Klakow *et al* for Coulomb systems [10, 11]. Usually Gaussian wave packets are employed. This reduces the time evolution of a complex wavefunction in a full N -body quantum description to the evolution of a few relevant parameters, such as positions, momenta and widths of the wave packet, and scales down the amount of numerical work from the solution of a partial differential equation to the much simpler case of a set of ordinary differential equations. Nevertheless there remains the formidable task of anti-symmetrization. It is implemented in our approach in terms of matrix inversions to which the calculation of expectation values of operators with Slater determinants can be reduced.

In this paper, we present in section 2 the theory of WPMD, paying particular attention to the anti-symmetrization of the many-body wavefunction. In section 3, we compare the results for the equation of state of hydrogen with experiments [13] and present our calculations of the Hugoniot of deuterium together with experiments [1, 2] and other theories [1, 4, 5, 8, 14, 15].

2. Theory of wave packet molecular dynamics

In our current application of the WPMD to hydrogen, the N protons of our simulation sample are described classically, i.e. by their positions \vec{R}_I and momenta \vec{P}_I , whereas the N electrons are represented by an anti-symmetrized product of one-particle wavefunctions $\varphi_k(\vec{x}_k)$:

$$\Psi(\vec{x}_1, \dots, \vec{x}_N) = \frac{1}{\sqrt{N! \det(\mathbf{O})}} \sum_{\sigma \in \mathcal{P}} \text{sgn}(\sigma) \prod_{k=1}^N \varphi_{\sigma_k}(\vec{x}_k). \quad (1)$$

Here, \mathcal{P} is the set of permutations of order N , and \mathbf{O} is the overlap matrix

$$O_{kl} := \langle \varphi_k | \varphi_l \rangle. \quad (2)$$

As an ansatz for the one-particle wavefunctions $\varphi_k(\vec{x})$ we take periodic Gaussian wave packets [7]:

$$\varphi_k(\vec{x}) \propto \sum_{\vec{n} \in \mathbb{Z}^3} \exp \left[- \left(\frac{3}{4\gamma_k^2} + \frac{i p \gamma_k}{2\hbar} \right) (\vec{x} - \vec{r}_k - \vec{n}L)^2 + \frac{i}{\hbar} \vec{p}_k (\vec{x} - \vec{r}_k - \vec{n}L) \right] \quad (3)$$

with the eight variational parameters $\{\vec{r}_k, \vec{p}_k, \gamma_k, p\gamma_k\}$.

Since the wavefunctions φ_k and the associated densities ρ_{kl} are periodic with a period of one box length L of the simulation cube, we can rewrite them in the Fourier representation [16]:

$$\varphi_k(\vec{x}) = \sum_{\vec{v} \in \mathbb{Z}^3} w_{\vec{v}}^k \exp \left(\frac{2\pi i}{L} \vec{v} \vec{x} \right) \quad (4)$$

$$\rho_{kl}(\vec{x}) := \varphi_k^*(\vec{x}) \varphi_l(\vec{x}) = \sum_{\vec{v} \in \mathbb{Z}^3} d_{\vec{v}}^{kl} \exp \left(\frac{2\pi i}{L} \vec{v} \vec{x} \right). \quad (5)$$

Here, the complex Fourier coefficients $w_{\vec{v}}^k$ of the wavefunctions depend only on the variational parameters and satisfy the normalization condition

$$1 = \int_{L^3} \varphi_k^*(\vec{x}) \varphi_k(\vec{x}) d^3x = L^3 \sum_{\vec{v} \in \mathbb{Z}^3} |w_{\vec{v}}^k|^2. \quad (6)$$

The Fourier coefficients $d_{\vec{v}}^{kl}$ of the densities can be expressed in terms of the coefficients $w_{\vec{v}}^k$ via

$$d_{\vec{v}}^{kl} = \sum_{\vec{\mu} \in \mathbb{Z}^3} (w_{\vec{\mu}}^k)^* w_{\vec{\mu} + \vec{v}}^l. \quad (7)$$

The Hamilton operator we use is given as $\hat{H} = \hat{H}_{\text{kin}} + \hat{H}_{\text{cou}} + \hat{H}_{\text{ext}}$ with

$$\hat{H}_{\text{kin}} = \sum_I \frac{P_I^2}{2M} + \sum_i \frac{\hat{p}_i^2}{2m} \quad (8)$$

$$\begin{aligned} \hat{H}_{\text{cou}} &= H_{\text{pp}} + \hat{H}_{\text{ee}} + \hat{H}_{\text{ep}} \\ &= \frac{e^2}{4\pi\epsilon_0} \left(\sum_{I < J} \frac{1}{|\bar{R}_I - \bar{R}_J|} + \sum_{i < j} \frac{1}{|\hat{x}_i - \hat{x}_j|} - \sum_{I,j} \frac{1}{|\bar{R}_I - \hat{x}_j|} \right) \end{aligned} \quad (9)$$

$$\hat{H}_{\text{ext}} = \frac{9\hbar^2}{8m\gamma_0^4} \sum_i (\hat{x}_i - \langle \hat{x}_i \rangle)^2. \quad (10)$$

Here, the indices I and J run over all protons, whereas the i and j run over all electrons in the system. M and m are the masses of the proton and of the electron, respectively.

To avoid an infinite growth of the widths γ_k of unbound electrons, we confine every wave packet in an external harmonic-oscillator potential \hat{H}_{ext} which moves together with the centre of mass of the electron and thus does not influence its motion. It can be interpreted physically as a constraint acting on the variance $\langle (\hat{x}_k - \langle \hat{x}_k \rangle)^2 \rangle$ of the wave packet. The constant Lagrangian parameter γ_0 adjusts the mean width of *unbound* electrons. To minimize the influence on *bound* wave packets, γ_0 is chosen much larger than the typical width of a bound electron, e.g. in an atom or molecule [17].

The expectation value of the kinetic and potential energies of the Slater sum (1) can be written in terms of the inverse overlap matrix $\mathbf{Y} = \mathbf{O}^{-1}$ (2) and the matrix elements $T_{kl} := \langle \varphi_k | \hat{H}_{\text{kin}} | \varphi_l \rangle$, $U_{kl} := \langle \varphi_k | \hat{H}_{\text{ep}} | \varphi_l \rangle$ and $V_{klmn} := \langle \varphi_k \varphi_l | \hat{H}_{\text{ee}} | \varphi_m \varphi_n \rangle$ [12]:

$$E_{\text{kin}} := \langle \Psi | \hat{H}_{\text{kin}} | \Psi \rangle = \sum_{kl} T_{kl} Y_{lk} = \text{Tr}(\mathbf{T}\mathbf{Y}) \quad (11)$$

$$E_{\text{cou,ep}} := \langle \Psi | \hat{H}_{\text{ep}} | \Psi \rangle = \sum_{kl} U_{kl} Y_{lk} = \text{Tr}(\mathbf{U}\mathbf{Y}) \quad (12)$$

$$E_{\text{cou,ee}} := \langle \Psi | \hat{H}_{\text{ee}} | \Psi \rangle = \sum_{klmn} V_{klmn} (Y_{mk} Y_{nl} - Y_{ml} Y_{nk}). \quad (13)$$

Calculating the matrix elements O_{kl} , T_{kl} , U_{kl} and V_{klmn} from the Fourier representation of the one-particle wavefunctions, equation (4), we obtain

$$O_{kl} = L^3 \sum_{\vec{v} \in \mathbb{Z}^3} (w_{\vec{v}}^k)^* w_{\vec{v}}^l = L^3 d_0^{kl} \quad (14)$$

$$T_{kl} = \frac{L}{2m} (2\pi\hbar)^2 \sum_{\vec{v} \in \mathbb{Z}^3} \vec{v}^2 (w_{\vec{v}}^k)^* w_{\vec{v}}^l \quad (15)$$

$$U_{kl} = -\frac{e^2}{4\pi\epsilon_0} \frac{L^2}{\pi} \sum_{\vec{v} \in \mathbb{Z}^3 \setminus \{0\}} \frac{1}{\vec{v}^2} d_{\vec{v}}^{kl} \sum_I \exp\left(\frac{2\pi i}{L} \vec{v} \cdot \bar{R}_I\right) \quad (16)$$

$$V_{klmn} = \frac{e^2}{4\pi\epsilon_0} \frac{L^5}{\pi} \sum_{\vec{v} \in \mathbb{Z}^3 \setminus \{0\}} \frac{1}{\vec{v}^2} d_{-\vec{v}}^{km} d_{\vec{v}}^{ln}. \quad (17)$$

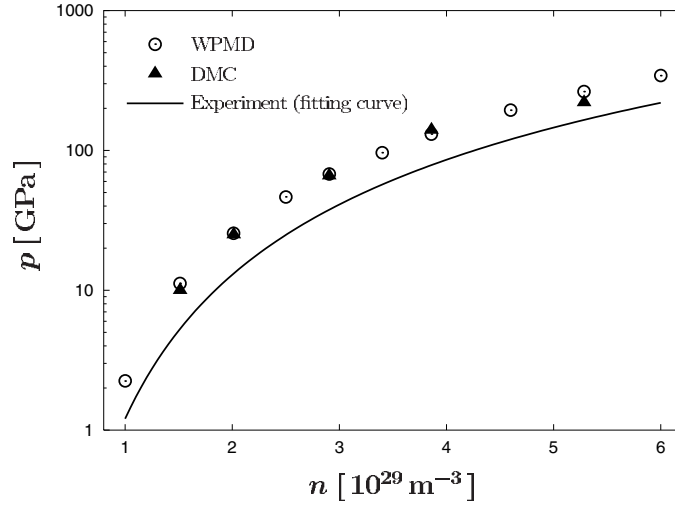


Figure 1. Equation of state of hydrogen at constant temperature $T = 300$ K. The WPMD result is compared with ‘fixed-node diffusion Monte Carlo’ (DMC) simulations [19] and diamond anvil experiments [13].

With the introduction of the matrices $\mathbf{D}_{\bar{\nu}} \equiv (d_{\bar{\nu}}^{kl})$, equations (13) and (17) lead to

$$E_{\text{cou,ee}} = \frac{e^2}{4\pi\epsilon_0} \frac{L^5}{\pi} \sum_{\nu \in \mathbb{Z}^3 \setminus \{0\}} \frac{1}{\nu^2} \left[\text{Tr}(\mathbf{D}_{-\bar{\nu}} \mathbf{Y}) \text{Tr}(\mathbf{D}_{\bar{\nu}} \mathbf{Y}) - \text{Tr}(\mathbf{D}_{-\bar{\nu}} \mathbf{Y} \mathbf{D}_{\bar{\nu}} \mathbf{Y}) \right]. \quad (18)$$

Formula (18) reduces the computational effort from calculating $N!$ terms of the Slater sum to one matrix inversion and several matrix products and scales like N^3 . Furthermore, the matrix inversion itself is numerically very stable and no problem with the alternating signs of the permutations occurs.

3. Results

We applied the WPMD method to the equation of state of hydrogen and deuterium. As we are interested here in equilibrium properties only, we did not propagate the system in time explicitly, but used a force-bias Monte Carlo algorithm [18] to simulate a canonical ensemble characterized by Gibb’s distribution. The number of particles was $2N = 108$ (54 protons and 54 electrons). The Lagrangian parameter γ_0 in \hat{H}_{ext} , see equation (10), was chosen as $\gamma_0 = 0.64\lambda_{\text{th}}$ with the thermal wavelength $\lambda_{\text{th}} = \hbar/(mk_B T)^{1/2}$. The pressure p of the system is extracted via the virial theorem

$$p = \frac{1}{3V} \left(2\langle \hat{H}_{\text{kin}} \rangle - \left\langle \sum_k \hat{\xi}_k \frac{\partial \hat{H}_{\text{pot}}}{\partial \hat{\xi}_k} \right\rangle \right) = \frac{2n}{3} (2E_{\text{kin}} - 2E_{\text{ext}} + E_{\text{cou}}) \quad (19)$$

where $\hat{\xi} = (\hat{x}_i, \vec{R}_i)$ is a $6N$ -dimensional vector composed of the operator \hat{x}_i and the proton coordinate \vec{R}_i , and $\hat{H}_{\text{pot}} = \hat{H}_{\text{cou}} + \hat{H}_{\text{ext}}$. $n = N/V$ is the number density of electrons and $E_{\text{kin}} = \langle \hat{H}_{\text{kin}} \rangle / (2N)$ etc are the mean energies per particle. The second equality of (19) holds because $\hat{H}_{\text{cou}} \propto |\hat{x}|^{-1}$ and $\hat{H}_{\text{ext}} \propto |\hat{x}|^2$. The last expression for the pressure in equation (19) also motivates the definition of a renormalized kinetic energy

$$\tilde{E}_{\text{kin}} := E_{\text{kin}} - E_{\text{ext}}. \quad (20)$$

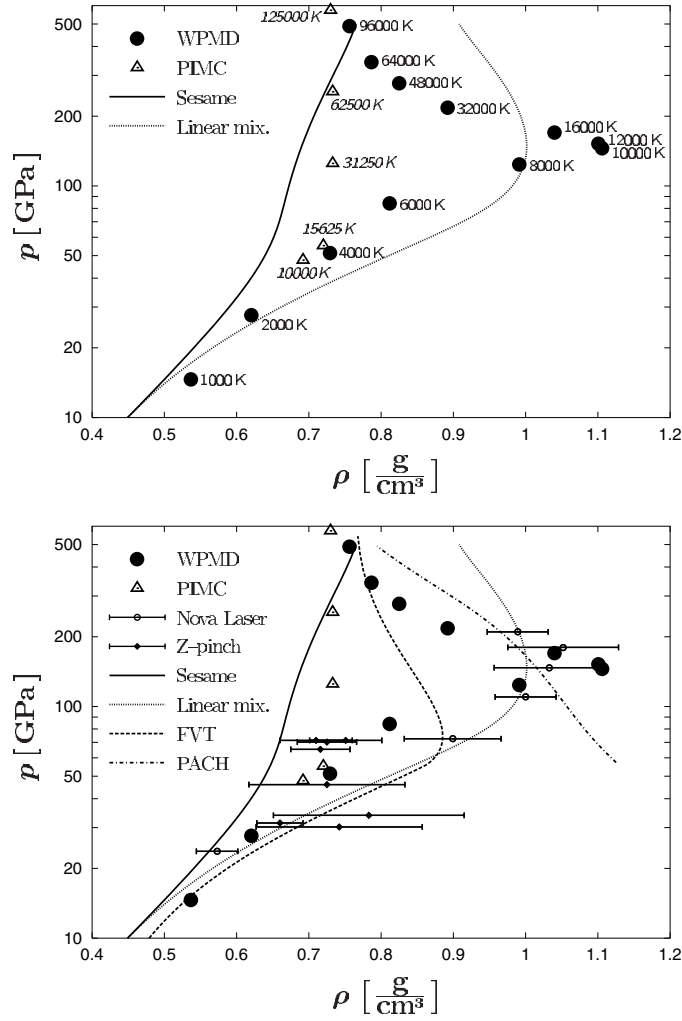


Figure 2. Equation of state of deuterium at constant Hugoniot. The WPMD result is compared with experiments with the Nova laser [1] and Z-pinches [2], with PIMC simulations [4], with the Sesame database [1] and the analytical models ‘linear mixing’ [1, 14], ‘FVT’ and ‘PACH’ [15, 8].

With this definition the virial theorem takes its well-known form for Coulomb systems $p = (2n/3)(2\tilde{E}_{\text{kin}} + E_{\text{cou}})$. In the high-temperature limit this yields the correct pressure $p = 2nk_{\text{B}}T = (2n/3)2\tilde{E}_{\text{kin}}$ for a completely dissociated and ionized ideal hydrogen plasma.

Work on the implementation of the full anti-symmetrization, namely of equation (18), is in progress. Presently the effects of the anti-symmetrization on the electron–electron interaction are still neglected, that is, the results presented here are obtained in the approximation where equations (13) and (18) are simplified to

$$E_{\text{cou,ee}} = \sum_{kl} V_{klkl} = \frac{e^2}{4\pi\epsilon_0} \frac{L^5}{\pi} \sum_{v \in \mathbb{Z}^3 \setminus \{0\}} \frac{1}{v^2} |\text{Tr}(\mathbf{D}_v)|^2. \quad (21)$$

Figure 1 shows the pressure of hydrogen as a function of density at a constant temperature $T = 300$ K. The excellent agreement of our WPMD model with ‘fixed-node diffusion Monte

Carlo' (DMC) simulations of [19] demonstrates that essential quantum effects are treated quite well in the WPMD scheme. The WPMD and DMC results also show qualitatively the same behaviour as observed in the diamond anvil experiments of Loubeyre *et al* [13]. The overall factor of about 1.75 between experiment and theories still, however, needs to be explained.

We also performed simulations of deuterium at a constant Hugoniot

$$E - E_0 + \frac{1}{2} \left(\frac{1}{n} - \frac{1}{n_0} \right) (p + p_0) = 0. \quad (22)$$

They actually run at a constant temperature, while the density was adjusted dynamically to fulfil equation (22), where $n_0 = 0.515 \times 10^{29} \text{ m}^{-3}$ is the initial number density of electrons, $p_0 \approx 0$ is the initial pressure and E_0 is the ground state energy per atom of the solid deuterium. Its exact value is $E_0 = -15.886 \text{ eV}$, whereas we have $E_0 \approx -13 \text{ eV}$ in the WPMD model.

The results are presented in figure 2 together with the shock-wave experiments [1, 2] and several theoretical approaches. Additional information on the corresponding temperatures is given for the WPMD and path-integral Monte Carlo (PIMC) models [4] in the upper part of figure 2. At pressures below 70 GPa, the equation of state at constant Hugoniot from the WPMD simulations is in good agreement with both the recent experiments of Knudsen *et al* [2] and most of the other theoretical results, e.g. the PIMC simulations, which predict, however, a much higher temperature at the same pressure (see the upper part of figure 2). The Hugoniot from the Sesame database is generally much stiffer, whereas the linear mixing model [5], the fluid variational theory (FVT) [15, 8] and the earlier laser-driven shock-wave experiments [1] show a larger compressibility. These differences are strongly magnified with increasing pressure where the Nova laser experiments found a significant higher density in the range of 73 GPa–210 GPa than many of the other approaches. Surprisingly, the WPMD shows a similar large, about sixfold, compression around 130 GPa.

4. Conclusions and outlook

We advanced the WPMD technique, which takes into account essential quantum effects such as the wave nature of the electrons and their indistinguishability, for applications to dense hydrogen. Using the WPMD method we calculated the equation of state of hydrogen and deuterium. Comparing with the experiments we see quite good agreement with the newer experiments with Z-pinchs at pressures below 70 GPa. At higher pressures the WPMD provides a similar large density as observed from the shock waves driven by the Nova laser.

In the realization of the WPMD model presented here we still neglected the effects of anti-symmetrization in the electron–electron interaction. The implementation of the full formula (18) is in progress. We anticipate in general a lowering of the pressure due to the additional exchange contributions and possibly a smoothing of the cusp in the Hugoniot equation of state at maximal compression.

Acknowledgments

This work was supported by the Bundesministerium für Bildung und Forschung (BMBF 06ER931).

References

- [1] DaSilva L B *et al* 1997 *Phys. Rev. Lett.* **78** 483
- [2] Knudson M D *et al* 2001 *Phys. Rev. Lett.* **87** 225501

-
- [3] Saumon D and Chabrier G 1992 *Phys. Rev. A* **46** 2054
 - [4] Militzer B and Ceperley D M 2000 *Phys. Rev. Lett.* **85** 1890
 - [5] Ross M 1998 *Phys. Rev. B* **58** 669
 - [6] Lenosky T J, Bickham S R, Kress J D and Collins L A 2000 *Phys. Rev. B* **61** 1
 - [7] Knaup M, Reinhard P-G, Toepffer C and Zwicknagel G 2002 *Comput. Phys. Commun.* **147** 202
 - [8] Juranek H, Redmer R and Rosenfeld Y 2002 *J. Chem. Phys.* **117** 1768
 - [9] Heller E J 1975 *J. Chem. Phys.* **62** 1544
 - [10] Klakow D, Toepffer C and Reinhard P-G 1994 *Phys. Lett. A* **192** 55
 - [11] Klakow D, Toepffer C and Reinhard P-G 1994 *J. Chem. Phys.* **101** 10766
 - [12] Feldmeier H 1990 *Nucl. Phys. A* **515** 147
 - [13] Loubeyre P *et al* 1996 *Nature* **383** 702
 - [14] Holmes N C, Ross M and Nellis W J 1995 *Phys. Rev. B* **52** 15835
 - [15] Juranek H, Redmer R and Stolzmann W 2001 *Contrib. Plasma Phys.* **41** 131
 - [16] Knaup M, Reinhard P-G and Toepffer C 2001 *Contrib. Plasma Phys.* **41** 159
 - [17] Knaup M, Reinhard P-G and Toepffer C 1999 *Contrib. Plasma Phys.* **39** 57
 - [18] Allen M P and Tildesley D J 1987 *Computer Simulation of Liquids* (Oxford: Clarendon)
 - [19] Ceperley D M and Alder B J 1987 *Phys. Rev. B* **36** 2092